Impact of limiting dimension on thermal conductivity of one-dimensional silicon phononic crystals

R. Yanagisawa, J. Maire, A. Ramiere, R. Anufriev, and M. Nomura

Citation: Appl. Phys. Lett. **110**, 133108 (2017); doi: 10.1063/1.4979080
View online: http://dx.doi.org/10.1063/1.4979080
View Table of Contents: http://aip.scitation.org/toc/apl/110/13
Published by the American Institute of Physics

Impact of limiting dimension on thermal conductivity of one-dimensional silicon phononic crystals

R. Yanagisawa,[1] J. Maire,[1,2] A. Ramiere,[1,2] R. Anufriev,[1] and M. Nomura[1,3,4,a)]
[1]*Institute of Industrial Science, The University of Tokyo, Tokyo 153-8505, Japan*
[2]*LIMMS, The University of Tokyo, Tokyo 153-8505, Japan*
[3]*Institute for Nano Quantum Information Electronics, The University of Tokyo, Tokyo 153-8505, Japan*
[4]*PRESTO, Japan Science and Technology Agency, Saitama 332-0012, Japan*

(Received 11 January 2017; accepted 6 March 2017; published online 31 March 2017)

We present experimental and theoretical investigations on the roles of the limiting dimensions, such as the smallest dimension, surface roughness, and density of holes in the reduction of thermal conductivity of one-dimensional phononic nanostructures at temperatures of 4 and 295 K. We discover that the thermal conductivity does not strongly depend on the period of the phononic crystal nanostructures whereas the surface roughness and the smallest dimension of the structure—the neck—play the most important roles in thermal conductivity reduction. Surface roughness is a very important structural parameter in nanostructures with a characteristic length less than 100 nm in silicon. The importance of the roughness increases as the neck size decreases, and the thermal conductivity of the structure can differ by a factor of four, reaching the thermal conductivity of a small nanowire. The experimental data are analyzed using the Callaway–Holland model of Boltzmann equation and Monte Carlo simulation providing deeper insight into the thermal phonon transport in phononic nanostructures. *Published by AIP Publishing.*
[http://dx.doi.org/10.1063/1.4979080]

Nanoscale heat transport attracts considerable attention owing to its characteristic physics, which differ completely from those of bulk materials,[1,2] and has practical importance for enhancing the efficiency of thermoelectric devices by reducing the thermal conductivity.[3,4] The heat conduction in nanostructures is significantly hindered by enhanced surface phonon scattering, which results in a very low thermal conductivity. Although silicon has poor thermoelectric performance owing to its high thermal conductivity, in the past decade, a dramatic reduction in thermal conductivity was demonstrated in silicon nanostructures,[5–9] making silicon a good thermoelectric material candidate.[10]

Recently, it was reported that nano-patterning of thin films with two-dimensional (2D) periodic arrays of holes, known as phononic crystals (PnCs), reduced the thermal conductivity because of strongly enhanced surface scattering.[11–18] Nevertheless, the efficiency of the surface scattering can be further enhanced by the increase in the surface area per unit volume and increase in the surface roughness. Such conditions can be met in one-dimensional (1D) PnCs, which may further decrease the thermal conductivity.

In this study, we experimentally investigated the heat transport in 1D PnCs using the microscale time-domain thermoreflectance (μ-TDTR) technique. We showed that the thermal conductivity was significantly decreased compared with that of unpatterned nanowires with identical dimensions. The experimentally obtained thermal conductivities were compared with the values calculated using the Callaway–Holland model to clarify the thermal phonon transport in the structures. Moreover, we discovered that the surface roughness increasingly affected the thermal conductivity as the characteristic length decreased. We studied the phonon mean free path (MFP) in 1D PnC nanostructures via the Monte Carlo method to demonstrate this.

We fabricated 1D PnCs on a commercial silicon-on-insulator wafer with a 145-nm-thick single crystalline silicon (100) top layer. First, $4 \times 4\ \mu m^2$, 125-nm-thick aluminum pads were deposited by electron-beam evaporation using an electron-beam lithography mask. Next, 1D arrays of holes were installed in the silicon top layer using a second electron-beam lithography mask and inductively coupled plasma reactive-ion etching (RIE) with SF_6/O_2 gases. Simultaneously, several strips were etched along the hole arrays to create 300-nm-wide and 10-μm-long nanowires on the two opposite sides of the aluminum pads. Finally, to suspend the structures, the buried SiO_2 layer was removed using vapor hydrofluoric acid. A single wafer contained several different samples, with periods of 300 and 600 nm and hole diameters in the range of 80–180 nm for each period, fabricated simultaneously under the same conditions, ensuring identical surface roughness for all of them. By changing the etching conditions of the RIE, we fabricated two sets of samples with high (rough) and low (smooth) surface roughness. Figure 1 shows typical scanning electron microscopy (SEM) images of our samples. The central silicon island with the aluminum pad was connected to the heat sink by ten PnC nanowires. Figures 1(b) and 1(c) show detailed images of 1D PnCs with periods of 300 and 600 nm, respectively. The roughness of the sidewalls was estimated to be 2.5 nm for the smooth samples and >10 nm for the rough samples by high-resolution SEM.

The samples were placed in a He-flow optical cryostat with a controllable temperature to perform measurements at

a)nomura@iis.u-tokyo.ac.jp

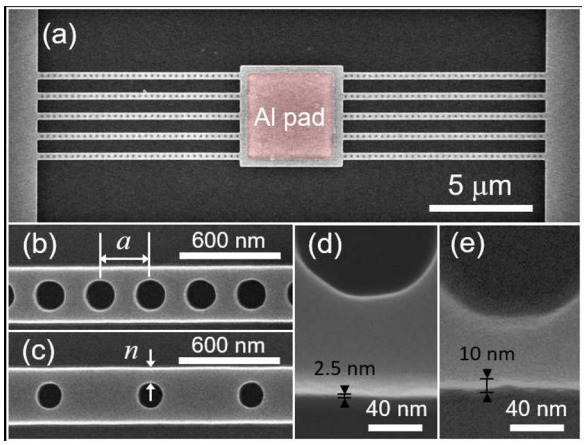

FIG. 1. SEM images of the samples. (a) Top view of a sample. (b) and (c) Close-up views of PnCs with periods of 300 and 600 nm; a is the period of the hole array; n is the neck size; and the width of all PnCs is fixed at 300 nm. (d) and (e) Sidewall roughness of smooth and rough PnCs, respectively.

4 and 295 K. The thermal contact between the sample and the cryostat was ensured by a thin layer of silicon grease so that the heat sink of the PnCs remained at the regulated temperature. The cryostat was under vacuum so that heat was dissipated only by conduction through the PnCs.

The in-plane thermal conductivity of the samples was determined using a custom-made μ-TDTR setup. The experimental setup consisted of two lasers—a probe laser and a pump laser—that were both focused on the central aluminum pad. The pump pulsed laser ($\lambda = 642$ nm) served as a heating pulse, with a duration and repetition rate of 500 ns and 1 kHz, respectively. The probe continuous-wave laser ($\lambda = 785$ nm) detected changes in the reflectivity of the aluminum pad, which were caused by variations in the temperature of the silicon underneath. After the heating pulse was applied, the heat diffusion through the PnCs resulted in an exponential decrease in the aluminum reflectivity. The thermal conductivity of the sample was derived from this measured decay curve, via comparison with a finite-element model in which the thermal conductivity of the PnC region was the free parameter. Further details regarding the experimental technique are presented in previous publications.[12,19,20]

Figure 2 shows the ratio of the PnC thermal conductivity to that of the unpatterned nanowires—$\kappa_{PnC}/\kappa_{unpatterned}$—as functions of both hole diameter and limiting dimension (neck size for PnCs and diameter for nanowires) for different periods, measured at 295 and 4 K. At both temperatures, we observed a reduction of the thermal conductivity with increasing hole size, which is consistent with previous experimental data.[12] In Figure 2, the filled circles show the thermal conductivity of the smooth samples, and the empty circles show that of the rough samples. The surface roughness played a significant role in the reduction of the thermal conductivity: the difference increased with the neck size and became as large as a factor of five at $n = 60$ nm at 4 K. Remarkably, the thermal conductivity was mostly independent of the period, in spite of the large difference in the porosity (25.8% and 14.8% for $a = 300$ nm with 172-nm-diameter holes and $a = 600$ nm with 184-nm-diameter holes, respectively).

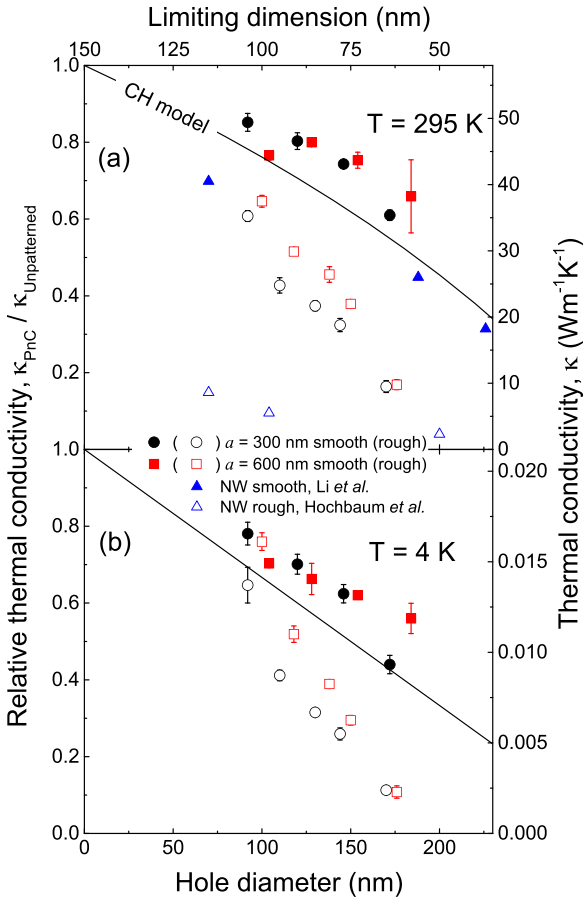

FIG. 2. Measured thermal conductivity of 1D PnCs and nanowires (NWs) as functions of the hole diameter and the limiting dimension (neck size for PnCs and diameter for nanowires) at (a) 295 K and (b) 4 K for $a = 300$ nm (black circles) and 600 nm (red squares). The left axis shows the thermal conductivity reduction compared with the unpatterned nanowire, and the right axis shows the absolute values of the thermal conductivity. The nanowire data of measured thermal conductivity reported by Li *et al.* (filled blue triangles) and Hochbaum *et al.* (empty blue triangles) are also plotted as a function of the limiting dimension.[6,22] The solid lines show the predictions of relative thermal conductivity by the Callaway–Holland model.

For both periods, at 295 K, the thermal conductivity reduction for the unpatterned nanowire exceeded 35% for the smooth samples with the largest holes. For the rough samples, the reduction exceeded 80% for both periods. This increased reduction is attributed to the strong phonon scattering on the nanowire surfaces and hole surfaces, which increased with the diameter. At 4 K, the reduction in the thermal conductivity reached 90% in the rough samples with the largest holes. Although the total number of holes was smaller in samples with longer periods, the impact of the period on the thermal conductivity was generally small and disappeared in samples with large hole diameters. This trend can be explained by the reduction in the neck size; the MFP of phonons is limited by the narrowest part of the sample,[20,21] and thus, the surface phonon scattering rate is increased by the presence of holes.

We compare the experimentally obtained thermal conductivities with values obtained by simulation using the Callaway–Holland model to understand the thermal conduction in the 1D PnCs. The thermal conductivity based on this model is given by[23,24]

$$\kappa_{CH} = \frac{1}{6\pi^2}\sum_j \int \frac{\hbar^2 \omega_j{}^2(q)}{k_B T^2} \frac{\exp\left[\frac{\hbar\omega_j(q)}{k_B T}\right]}{\left(\exp\left[\frac{\hbar\omega_j(q)}{k_B T}\right]-1\right)^2} \times v_j(q)^2 \tau_j(q,T) q^2 dq, \quad (1)$$

where $\hbar$ is the reduced Planck's constant; k_B is the Boltzmann constant; T is the temperature; $\omega(q)$ and $v(q)$ are the angular frequency and the group velocity, respectively, at the wave vector q, taken from the bulk phonon dispersion relation; modifications of phonon dispersion due to downsizing and periodicity are not taken into account, as their impact at considered temperatures is relatively weak.[25,26] The scattering time τ is determined by three different scattering mechanisms—Umklapp, impurity, and boundary scattering—combined via Mattheissen's rule

$$\frac{1}{\tau} = \frac{1}{\tau_U} + \frac{1}{\tau_I} + \frac{1}{\tau_B}, \quad (2)$$

where the scattering time is defined as $\tau_U = AT\omega^2 \exp(-\theta/T)$ for Umklapp scattering, $\tau_I = B\omega^4$ for impurity scattering, and $\tau_B = C/v$ for diffusive boundary scattering. We use $A = 1.40 \times 10^{-19}$, $B = 1.32 \times 10^{-45}$, and $\theta = 152$ K, as reported by Hopkins *et al.*, for the thermal conductivity of the bulk.[27] The parameter C is the limiting dimension of the structure, which we set equal to the neck size, as the neck size is known to be approximately the limit for the MFP in PnCs.[20,21]

For comparison, in Fig. 2, we also plot literature data on silicon nanowires with diameters as the limiting dimension. The comparison shows that the model has the same trend as the experimental results for smooth 3-μm-long nanowires measured by Li *et al.*,[22] whose length is long enough to confirm the non-ballistic transport;[28] however, the theoretical curve was slightly below the actual values for the smooth PnCs. This difference can be explained by the fact that the Callaway–Holland model does not consider specular phonon scattering, causing some phonons to have an MFP longer than the neck size. However, rough PnCs, as well as the rough 2-μm-long nanowires measured by Hochbaum *et al.*,[6] have a lower thermal conductivity than that predicted by the model. This can be explained by the strong backscattering induced by the rough surfaces. For this reason, as the neck size of the rough samples was reduced, the thermal conductivity decreased towards the value measured for rough nanowires[6] with a corresponding diameter. Interestingly, as the hole diameter increased, the rough sidewalls appeared to play an increasingly important role in reducing the thermal conductivity.

To gain further insight into the physical phenomena occurring in the 1D PnCs, we performed 2D Monte Carlo simulations of the 4 K measurements. Phonon propagation in nanostructures at low temperatures can be described by the semi-ballistic transport regime, where boundary scattering is the main heat-diffusion phenomenon.[29] The fabrication imperfections create a surface roughness of a few nanometers, which, according to Soffer's theory,[30] leads to diffuse scattering for most scattering events in the main range of the phonon spectrum. Consequently, after each collision, the phonon is resampled in a random direction. The distance between two diffusions defines one MFP l_i. All such MFPs are sorted into ranges $[l_i - \delta l/2; l_i + \delta l/2]$, with $\delta l = 2$ nm. The MFP distribution is then computed by counting the number of MFPs in each range. To ensure good statistics, we simulate the trajectories of millions of phonons, where each phonon undergoes a few thousand collisions in the PnC. Because the number of collisions changes with the period and hole diameter, we normalized the MFP distribution by the total number of collisions ($N = \sum i$) to compare the different geometries.

Figures 3(a) and 3(b) show the normalized MFP distribution for periods of 300 and 600 nm, respectively, for hole diameters d of 80, 140, and 200 nm. Each curve has two main peaks: the first peak corresponds to the neck and the second peak corresponds to the nanowire width. As the hole diameter increased, the amplitudes of the neck peak and the nanowire peak increased and decreased, respectively, indicating that the neck size had an increasing influence on the MFP distribution. For the period of 300 nm, the relative importance of the neck compared to the nanowire peak

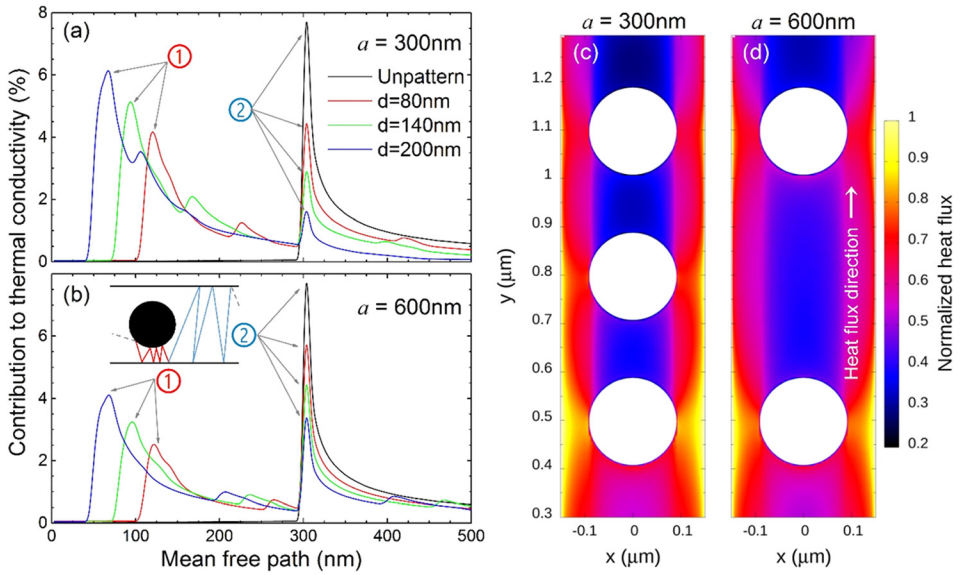

FIG. 3. Phonon MFP spectra in 1D PnCs with periods of (a) 300 and (b) 600 nm, calculated using the Monte Carlo method. (c) and (d) Normalized heat-flux map for 1D PnC with periods of 300 and 600 nm in the steady state, showing the higher concentration of energy in the necks.

increases up to a factor of four for the largest hole diameter of 200 nm, and even for the smallest hole diameter of 80 nm, the neck peak is as important as the nanowire peak; thus, phonons are mainly scattered at the sidewall around the neck and the neck size contributed significantly to the thermal conductivity. For the period of 600 nm, only hole diameters greater than 140 nm yielded a neck peak higher than the nanowire peak. Nevertheless, the neck peak was significantly wider and had a longer tail than the nanowire peak; accordingly, the neck size was the main limitation of the MFP and thus the thermal conductivity.

To complete the information provided by the MFP spectra, Figures 3(c) and 3(d) display the normalized heat flux maps in 1D PnCs with periods of 300 and 600 nm, respectively, calculated by Monte Carlo simulations around the first three or two holes closest to the heat source. The energy was clearly concentrated at the necks of the structures owing to the large number of hole-edge interactions. In other words, phonon localization appeared at the neck, especially for low-frequency phonons, which have long MFPs and contribute to a large part of thermal conductivity, leading to strong reduction of thermal conductivity. Similar localizations are reported in nanoscale PnCs, where the thermal conductivity of PnC dramatically decreased from the bulk.[31,32] Furthermore, phonons escaping the first neck were particularly oriented parallel to the y-axis and thus rarely went between the first and second holes. This effect was cumulative with the succession of holes; after a few holes, the heat propagated almost only through the passage left by the neck, which strongly reduced the impact of the periodicity of the holes. As shown in Figure 2, the heat conduction of the 1D PnC became comparable to that of a thin nanowire whose diameter corresponds to the neck size of the PnCs.

At room temperature, bulk phonon MFPs range from nanometer to millimeters, but in nanostructures, the MFPs are limited by the characteristic size of the structure.[20,21] At the temperature of 4 K, bulk phonon MFPs become substantially longer[33] because of reduced Umklapp scattering processes but remain approximately limited by the neck in the nanostructure. A larger part of the MFP distribution is thus blocked at 4 K, resulting in a larger reduction in the thermal conductivity.

In conclusion, we studied the impact of the nano-patterning and surface roughness on the thermal conductivity of 1D PnCs. In the smooth PnCs, the geometry—neck size—reduced the thermal conductivity by as much as 40% at room temperature and 50% at 4 K compared with an unpatterned nanowire. To better understand this result, the role of the limiting dimensions in PnCs was studied by Monte Carlo simulations. The simulations showed that the influence of the neck on phonon MFP increases and even dominates as the neck size is reduced below 100 nm. In this case, the thermal energy becomes localized in the narrow neck regions; thus, the surface roughness naturally becomes more important. This finding seems to be in agreement with our experimental data on rough PnC samples, in which the impact of the roughness increased as the neck was reduced. Thus, the surface roughness is an important structural parameter nanostructure with limiting dimensions of less than 100 nm.

Thus, on one hand, reduction of thermal conductivity by nano-patterning is limited by the minimum realistic neck size that can be fabricated by conventional top-down approach; on the other hand, surface roughness efficiently reduces thermal conductivity only in relatively small or narrow structures. However, our results show that surface roughness and nano-patterning combined together can reduce thermal conductivity of nanostructures much more efficiently than each of these mechanisms individually. This hybrid approach allows the thermal conductivity of our samples to match that of fragile as-grown nanowires or ultra-thin films, without a need to sacrifice the rigidity of the structure, and thus can significantly improve the performance and reliability of silicon thermoelectric devices.

This work was supported by the Project for Developing Innovation Systems of the MEXT, Japan, Kakenhi (15H05869 and 15K13270), PRESTO JST (JPMJPR15R4) and the Postdoctoral Fellowship of the Japan Society for the Promotion of Science.

[1]D. G. Cahill, W. K. Ford, K. E. Goodson, G. D. Mahan, A. Majumdar, H. J. Maris, R. Merlin, and S. R. Phillpot, J. Appl. Phys. **93**, 793 (2003).
[2]D. G. Cahill, P. V. Braun, G. Chen, D. R. Clarke, S. Fan, K. E. Goodson, P. Keblinski, W. P. King, G. D. Mahan, A. Majumdar, H. J. Maris, S. R. Phillpot, E. Pop, and L. Shi, Appl. Phys. Rev. **1**, 11305 (2014).
[3]G. J. Snyder and E. S. Toberer, Nat. Mater. **7**, 105 (2008).
[4]Z. Tian, S. Lee, and G. Chen, J. Heat Transfer **135**, 61605 (2013).
[5]A. I. Boukai, Y. Bunimovich, J. Tahir-Kheli, J.-K. Yu, W. A. Goddard III, and J. R. Heath, Nature **451**, 168 (2008).
[6]A. I. Hochbaum, R. Chen, R. D. Delgado, W. Liang, E. C. Garnett, M. Najarian, A. Majumdar, and P. Yang, Nature **451**, 163 (2008).
[7]E. Chávez-Ángel, J. S. Reparaz, J. Gomis-Bresco, M. R. Wagner, J. Cuffe, B. Graczykowski, A. Shchepetov, H. Jiang, M. Prunnila, J. Ahopelto, F. Alzina, and C. M. Sotomayor-Torres, APL Mater. **2**, 12113 (2014).
[8]P. Ferrando-Villalba, A. F. Lopeandia, L. Abad, J. Llobet, M. Molina-Ruiz, G. Garcia, M. Gerbolès, F. X. Alvarez, A. R. Goñi, F. J. Muñoz-Pascual, and J. Rodríguez-Viejo, Nanotechnology **25**, 185402 (2014).
[9]Y. S. Ju, Appl. Phys. Lett. **87**, 153106 (2005).
[10]M. Haras, V. Lacatena, F. Morini, J. F. Robillard, S. Monfray, T. Skotnicki, and E. Dubois, Mater. Lett. **157**, 193 (2015).
[11]J. Lim, H.-T. Wang, J. Tang, S. C. Andrews, H. So, J. Lee, D. H. Lee, T. P. Russell, and P. Yang, ACS Nano **10**, 124 (2016).
[12]R. Anufriev, J. Maire, and M. Nomura, Phys. Rev. B **93**, 45411 (2016).
[13]J. Tang, H.-T. Wang, D. H. Lee, M. Fardy, Z. Huo, T. P. Russell, and P. Yang, Nano Lett. **10**, 4279 (2010).
[14]J.-K. Yu, S. Mitrovic, D. Tham, J. Varghese, and J. R. Heath, Nat. Nanotechnol. **5**, 718 (2010).
[15]P. E. Hopkins, C. M. Reinke, M. F. Su, R. H. Olsson, E. A. Shaner, Z. C. Leseman, J. R. Serrano, L. M. Phinney, and I. El-Kady, Nano Lett. **11**, 107 (2011).
[16]N. Zen, T. A. Puurtinen, T. J. Isotalo, S. Chaudhuri, and I. J. Maasilta, Nat. Commun. **5**, 3435 (2014).
[17]M. Nomura, Y. Kage, D. Müller, D. Moser, and O. Paul, Appl. Phys. Lett. **106**, 223106 (2015).
[18]E. Dechaumphai and R. Chen, J. Appl. Phys. **111**, 73508 (2012).
[19]J. Nakagawa, Y. Kage, T. Hori, J. Shiomi, and M. Nomura, Appl. Phys. Lett. **107**, 23104 (2015).
[20]M. Nomura, Y. Kage, J. Nakagawa, T. Hori, J. Maire, J. Shiomi, R. Anufriev, D. Moser, and O. Paul, Phys. Rev. B **91**, 205422 (2015).
[21]A. Jain, Y.-J. Yu, and A. J. H. McGaughey, Phys. Rev. B **87**, 195301 (2013).
[22]D. Li, Y. Wu, P. Kim, L. Shi, P. Yang, and A. Majumdar, Appl. Phys. Lett. **83**, 2934 (2003).
[23]J. Callaway, Phys. Rev. **113**, 1046 (1959).
[24]M. G. Holland, Phys. Rev. **132**, 2461 (1963).

[25]J. Maire, R. Anufriev, R. Yanagisawa, A. Ramiere, S. Voltz, and M. Nomura, e-print, arXiv:1508.04574v2 [cond-mat.mes-hall] (2016).
[26]J. Lee, W. Lee, G. Wehmeyer, S. Dhuey, D. L. Olynick, S. Cabrini, C. Dames, J. J. Urban, and P. Yang, Nat. Commun. **8**, 14054 (2017).
[27]P. E. Hopkins, P. T. Rakich, R. H. Olsson, I. F. El-kady, and L. M. Phinney, Appl. Phys. Lett. **95**, 161902 (2009).
[28]J. Maire, R. Anufriev, and M. Nomura, Sci. Rep. **7**, 41794 (2017).
[29]A. Ramiere, S. G. Volz, and J. Amrit, J. Phys. D: Appl. Phys. **49**, 115306 (2016).
[30]S. B. Soffer, J. Appl. Phys. **38**, 1710 (1967).
[31]L. Yang, N. Yang, and B. Li, Nano Lett. **14**, 1734 (2014).
[32]D. Ma, H. Ding, H. Meng, L. Feng, Y. Wu, J. Shiomi, and N. Yang, Phys. Rev. B **94**, 165434 (2016).
[33]K. T. Regner, D. P. Sellan, Z. Su, C. H. Amon, A. J. H. McGaughey, and J. Malen, Nat. Commun. **4**, 1640 (2013).